Effects of Low Energy Muons on Electronics: Physical Insights and Geant4 Simulation

Sébastien Serre, Serguei Semikh, Jean-Luc Autran, Daniela Munteanu, Gilles Gasiot, Philippe Roche

Effects of Low Energy Muons on Electronics: Physical Insights and Geant4 Simulation

S. Serre, S. Semikh, J.L. Autran, D. Munteanu, G. Gasiot, P. Roche

***Abstract*–The impact of low energy (< 1 MeV) muons on electronics is studied from a physical point-of-view and investigated by numerical simulation using a new release of the TIARA code fully rewritten using the Geant4 toolkit. The effects of both direct ionization and negative muon capture mechanisms on the soft error occurrence in a 65nm CMOS SRAM are carefully examined and discussed.**

***Index Terms*— Atmospheric muon, negative muon capture, Geant4, Soft-Error, Single Event Upset, Monte Carlo simulation, SRAM.**

I. Introduction

ATMOSPHERIC muons represent an important part of the natural radiation constraint at ground level. Muons belong to the Meson or "hard" component in the atmospheric cosmic ray cascades and are the products of the decay of charged pions (charged mesons π^+ and π^-) via the weak interaction. In spite of their short lifetime but because they are relativistic, these particles are easily able to penetrate the atmosphere; they constitute the most preponderant charged particles at sea level. Muons are charged particles; both negative and positive muons can loss their kinetic energy by ionization process when they travel through matter. But this interaction with matter is tenuous and muons can travel large distances in matter, thus deeply penetrating into material circuits.

Up to now, the effect of muons on electronics has resulted in only a very small number of works. We can cite the pioneer work in the 80's of Ziegler and Lanford [1] and a few experimental characterization studies of memories (SRAM, DRAM) using artificial muon beams [2-4]. Recently, Sierawski et al. [5-6] conducted the first major work on the subject, combining measurements and numerical simulations on the effect of low energy (<3 MeV) and atmospheric positive muons on advanced technologies. They demonstrated and quantified the effects of muon direct ionization, evidencing a significant increase in the soft error rate (SER) for technologies with a critical charge typically below 0.2 fC (corresponding to the 22 nm technological node and beyond).

In the present work, we would like to explore, by simulation, the complementary effect of low energy (<1 MeV) *negative muons* on SRAM memories and evidence the importance of the *negative muon capture* mechanism as an additional mechanism of charge deposition for negative muons that can be stopped in silicon. Our study was conducted in three steps that correspond to the different sections of the present paper: in Section II, we review the physics of muon interactions with matter and silicon ; Section III details the development of the new version of our TIARA simulation code able to considering muon particles and finally in Section IV, we present and discuss our Monte Carlo simulations evidencing the effects of negative muons on the SEU occurrence in CMOS 65 nm SRAM.

Manuscript received September 28, 2012. This work is supported by the CATRENE Project # CA303 OPTIMISE (OPTImisation of MItigations for Soft, firm and hard Errors) and by the French Ministry of Economy under research convention #092930487.

S. Serre, S. Semikh, J.L. Autran and D. Munteanu are with Aix-Marseille University and CNRS, Institute of Materials, Microelectronics and Nanosciences of Provence (IM2NP, UMR CNRS 7334), Bâtiment IRPHE, 49 rue Joliot Curie, BP146, F-13384 Marseille Cedex 13, France (phone: +33 413552017, fax: +33 413552001, e-mail: jean-luc.autran@univ-amu.fr).

G. Gasiot and P. Roche are with STMicroelectronics, 850 rue Jean Monnet, F-38926 Crolles Cedex, France (e-mail: philippe.roche@st.com).

II. Theoretical Background

A. Interactions of muons with matter

The muon is an elementary particle similar to the electron, with a unitary negative electric charge and a mass about 200 times the mass of an electron. The muon, denoted by μ^- and also called "negative muon", has a corresponding antiparticle of opposite charge and equal mass: the antimuon, often called "positive muon" (μ^+). Both negative and positive are unstable particles with a mean lifetime of 2.2 μs. Independently of any interaction with matter, they spontaneously decay into three particles:

$$\mu^- \rightarrow e^- + \overline{\upsilon}_e + \upsilon_\mu$$
$$\mu^+ \rightarrow e^+ + \upsilon_e + \overline{\upsilon}_\mu \qquad (1).$$

Ziegler and Lanford have been the first authors to point out precisely how muons can interact with matter at relatively low incident primary energies [1]. They decompose the interaction into three primary processes:

1) *Muon direct ionization wake*. A charged muon loses its kinetic energy passing through semiconductor material by excitation of bound electrons and frees electron-hole pairs along its path as a result.
2) *Electromagnetic scattering* which induces energetic coulomb silicon nucleus recoil.
3) *Capture* of the negative muons by atomic nuclei when they are quasi stopped in matter. This complex capture mechanism releases recoiling heavy nuclei with a simultaneous emission of light particles (neutrons, protons, deuterons, α-particles, etc.).

In the present work, we will focus on this last mechanism which is at the origin of the production of large particle showers in matter. This section precisely reviews how a negative muon interacts weakly with a target nucleus and what are the conditions required to reach this type of interaction.

In general way, thenceforward that a negative muon rapidly slows down in stopping target material, it can be captured in an outer atomic orbit. Fast electromagnetic cascades ensue, bringing the muon down to the innermost 1s Bohr level orbit. Afterwards, the muon waits for its disappearance, either by decay or by nuclear capture as the muon comes closer to the nucleus [7-8]. More precisely:

- Thenceforth that the energy of the incoming muon is upper than 2 keV, the muon velocity is greater than the velocity of the valence electrons (Bohr velocity) and the muon crossing the target material knocks out electrons.
- In the low energy phase (lower than 2 keV) to rest, the muon velocity is less than that of the valence electrons: muon can exchange energy with the degenerate electron gas in arbitrarily small steps, and rapidly (in about $\sim 10^{-13}$ s) come to a stop.
- Once the muon reaches a state of no kinetic energy, it is captured by the host atom into high orbital momentum states, forming a *muonic atom*. Since all low-lying muonic states are unoccupied, the muon electromagnetic cascades down rapidly to the lowest quantum state (1s) available. Fermi and Teller showed that the time taken by a muon trapped in an atom to cascade down to the lowest Bohr orbit (1s) is negligible compared to its natural lifetime [9].
- After the muon has reached the 1s orbit, it either decays or gets captured by the nucleus via the weak interaction. Around Z = 11, the capture probability is approximately equal to the decay probability. In heavy nuclei (Z ~50), the ratio of capture to decay probabilities is about 25. In the highly interesting case of silicon for microelectronics (Z = 14), the ratio of capture to decay probabilities has been evaluated between 1.72 and 1.93 [10].

Historically, the study of the nuclear muon capture can be said to have truly begun with the paper by Tiomno and Wheeler [11]. As a result of the weak interaction the following nuclear reaction occurs:

$$\mu^- + \mathrm{A}_Z^N \rightarrow \nu_\mu + \mathrm{X} \qquad (2)$$

where the detectable product X consists of a residual heavy nucleus and light particles. The mean excitation energy in the nuclear muon capture is around 15 to 20 MeV. This is well above the nucleon emission threshold in all complex nuclei. Thus, the daughter nucleus (A, Z−1) can de-excite by emitting one or more neutrons, or charged light particles, besides via the electromagnetic mode [7]. In intermediate and heavy nuclei, the light particles are neutrons and/or γ rays in most of the cases. The few percents of charged light particles observed are mainly protons, but deuterons and α-particles have also been observed in still smaller quantities. Charged particle emission is more probable for light nuclei than for heavy nuclei.

Among all the possible channels of nuclear muon capture reactions, the neutron emission is the preferential one. This emission of neutrons can be approximately classified as direct or from an intermediate "compound nucleus" formed after the muon capture process. Direct emission refers to the neutron created in the elementary process:

$$\mu^- + p \rightarrow n + \nu_\mu \qquad (3)$$

which succeeds in leaking out of the nucleus. These neutrons have fairly high energies, from few MeV to as high as 40-50 MeV [12]. Most of the neutrons emitted after capture seem however to be "evaporation neutrons". In intermediate and heavy nuclei, the excitation energy acquired by the neutron formed in the capture process is shared with the other nucleons of the nucleus and a "compound nucleus" is formed. The intermediate excited nuclear state then loses energy by boiling-off mainly low-energy neutrons (with γ-rays) till a ground state is reached [7].

The following physical picture involving a two-step process can be used: the muon is captured by a quasi-free nucleon, whose acquired energy is distributed among the nucleons of the nucleus, and a compound nucleus is thus formed:

$$\mu^- + \mathrm{A}_Z^N \rightarrow \nu_\mu + (\mathrm{A}_{Z-1}^{N+1})^* \qquad (4)$$

The excited nuclear state then loses energy by evaporating nuclear particles (mainly neutrons) and γ-rays till a ground state is reached.

B. Negative muon capture in silicon

When negative muons stop in silicon, about 35% in average decay into an electron and two neutrinos. The remaining 65% are captured [Suzuki, 1987]. If an intermediate state is assumed, the reaction is:

$$\mu^- + {}^{28}\mathrm{Si} \rightarrow {}^{28}\mathrm{Al}^* + \nu_\mu + 100.5\ \mathrm{MeV} \qquad (5)$$

Sobottka et al. [13] have measured the energy spectrum for charged particle emission resulting after muon capture in ^{28}Si following some modes of de-excitation of ^{28}Al recoiling nucleus:

$$\begin{aligned} {}^{28}\mathrm{Al}^* &\rightarrow {}^{27}\mathrm{Al} + n\ (12.4\ \mathrm{MeV}) \\ &\rightarrow {}^{27}\mathrm{Mg} + p\ (14.2\ \mathrm{MeV}) \\ &\rightarrow {}^{24}\mathrm{Na} + \alpha\ (15.5\ \mathrm{MeV}) \\ &\rightarrow {}^{26}\mathrm{Mg} + d\ (18.4\ \mathrm{MeV}) \end{aligned} \qquad (6)$$

where the energy listed with each final state is the ground-state energy with respect to the ^{28}Si ground state.

According to the compilation of several works [12-17], among all the muons that are captured, 28% result in no particle emission, 15% result in charged particle emission (~10% protons, 5% deuterons and <1% tritons or α-particles – in some cases, there may be several percents of alpha-particles), 67% result in neutron emission, with 10% emission of both charged particles and neutrons.

Finally, Measday [18] has suggested a global pattern of muon-capture reactions for ^{28}Si, expressed as a percentage of all captures. These results are reported in Table I and give an exhaustive view of the negative muon capture in silicon. Such a capture is thus able to produce secondary heavy nuclei that

TABLE I. GLOBAL PATTERN FOR NEGATIVE MUON CAPTURE REACTIONS IN ^{28}SI TARGET MATERIAL. AFTER [18].

Reaction	***%***	***Reaction***	***%***
$(\mu^-,\nu)^{28}$Al	26	$(\mu^-,\nu p)^{27}$Mg	2.0
$(\mu^-,\nu n)^{27}$Al	45	$(\mu^-,\nu pn)^{26}$Mg	4.9
$(\mu^-,\nu 2n)^{26}$Al	12	$(\mu^-,\nu p2n)^{25}$Mg	1.4
$(\mu^-,\nu 3n)^{25}$Al	1	$(\mu^-,\nu p3n)^{24}$Mg	0.6
		$(\mu^-,\nu p4n)^{23}$Mg	0.1
$\Sigma(n)$	**84**	**$\Sigma(p)$**	**9.0**

Reaction	***%***	***Reaction***	***%***
$(\mu^-,\nu d)^{26}$Mg	3.1	$(\mu^-,\nu 2pn)^{25}$Na	0.1
$(\mu^-,\nu dn)^{25}$Mg	1.0	$(\mu^-,\nu\alpha)^{24}$Na	1.0
$(\mu^-,\nu d2n)^{24}$Mg	0.3	$(\mu^-,\nu\alpha n)^{23}$Na	0.8
		$(\mu^-,\nu\alpha 2n)^{22}$Na	0.5
		$(\mu^-,\nu\alpha 3n)^{21}$Na	0.2
$\Sigma(d)$	**4.4**	**Σ(Na)**	**2.6**

can deposit important charge in silicon; one of the objectives of this study, detailed in the following, is precisely to study by simulation the importance of this capture mechanism on the soft-error occurrence in a static memory circuit.

III. TIARA-G4 MONTE CARLO SIMULATION CODE

A. Code architecture and migration towards Geant4

In order to accurately simulate the interaction of muons with ICs, and more generally the impact of atmospheric charged particles (muons, protons, pions), a new version of the TIARA code [19-20] has been developed. This new version is called TIARA-G4, in reference to the fact that it is totally rewritten in C++ using Geant4 classes and libraries and compiled as a full Geant4 application [21]. The main improvement of TIARA-G4 with respect to the first version of the code comes precisely from this transformation of the code in a Geant4 application, allowing the use of Geant4 classes for the description of the circuit geometry and materials (now including the true BEOL structure) and the integration of the particle transport and tracking directly in the simulation flow, without the need of external databases or additional files.

Figure 1 shows the flowchart of TIARA-G4 and the link between the different modules with Geant4 classes, libraries and other additional extensions. Schematically, the complete simulation chain is partitioned into five main code modules, briefly described in the following:

1) Circuit architecture construction module: the structure creation in TIARA-G4 is based on 3D circuit geometry information extracted from GDS formatted data classically used in the Computer-Aided Design (CAD) flow of semiconductor circuit manufacturing. To perform such an extraction from the GDS layout description, a separate tool has been developed [22]. It parses the GDS file, obtains coordinate points of CAD layers and using geometrical computations tracks the positions and dimensions of the transistor active areas, cell dimensions, p-type and n-type and Back-End-Of-Line (BEOL) stack geometry. Based on this information and additional data concerning the depth of the wells, junctions, STI regions (obtained from TCAD or SIMS measurements) and BEOL layer composition, TIARA creates a 3D structure of the elementary memory cell and, by repetition, of the complete portion of the simulated circuit. The real 3D geometry is simplified since it is essentially based on the juxtaposition of boxes of different dimensions, each box being associated to a given material (silicon, insulator, metal, etc.) or doped semiconductor (p-type, n-type).

2) Radiation event generator module: to numerically generate the particles with the spectral, spatial and angular distributions chosen by the user, we use the G4 General Particle Source (GPS) [23] which is part of the Geant4 distribution. The module allows the user to define all the source parameters, in particular the energy of the emitted particles from a given energy distribution defined in a separate input file.

3) Interaction, transport and tracking module: once an incident particle has been numerically generated with the radiation event generator, the Geant4 simulation flow computes the interactions of this particle with the target (the simulated circuit) and transports step-by-step the particle and all the secondary particles eventually produced inside the world volume (the largest volume containing, with some margins, all other volumes contained in the circuit geometry). The transport of each particle occurs until the particle loses its kinetic energy to zero, disappears by an interaction or comes to the end of the world volume. The G4ProcessManager class contains the list of processes that a particle can undertake. A physical process describes how particles interact with materials. In TIARA-G4, the physical list QGSP_BIC_HP [24] is used; this list includes binary cascade, precompound and various de-excitation models for hadrons standard EM, with high precision neutron model used for neutrons below 20 MeV. For muons, the specific classes and models considered are given in paragraph III.B below.

4) Circuit electrical response module: this portion of the code evaluates the electrical response of the circuit subjected to the irradiation. At the end of a given simulation sequence dedicated to particle interactions and transportation,TIARA-G4 examines the tracks of all the charged particles involved in this simulation step (including eventually the track of the incident primary particle if it is charged) and determine the complete list of the different silicon volumes (drains, Pwells, Nwells, substrates, etc.) traversed by these particles. The electrical response of the circuit is then evaluated following a dedicated model and using one or several criteria as a function of the circuit nature and architecture. In section III.C, we detail the criteria used to evaluate a single event upset in a SRAM circuit.

5) Soft Error Rate Calculation Module: at the end of the simulation flow, the last module of the TIARA-G4 code evaluates the Soft Error Rate (SER) of the simulated circuit and write in a series of file all the simulation results in terms of error bitmap and signatures, circuit cross-section, etc.

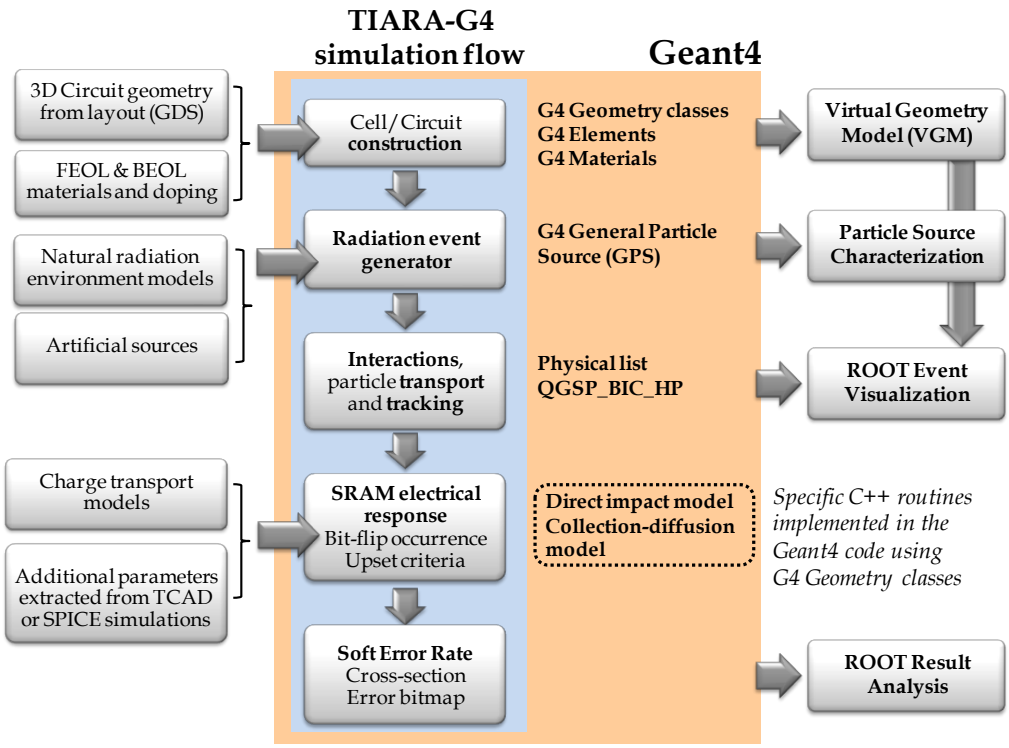

Figure 1. Flowchart of the TIARA-G4 simulation code. This new code release is compiled as a full Geant4 application covering the complete simulation chain, from circuit construction to soft-error rate final calculation. The main inputs/outputs, the major modules within the internal simulation flow as well as the links with Geant4 classes and external modules/programs are also indicated.

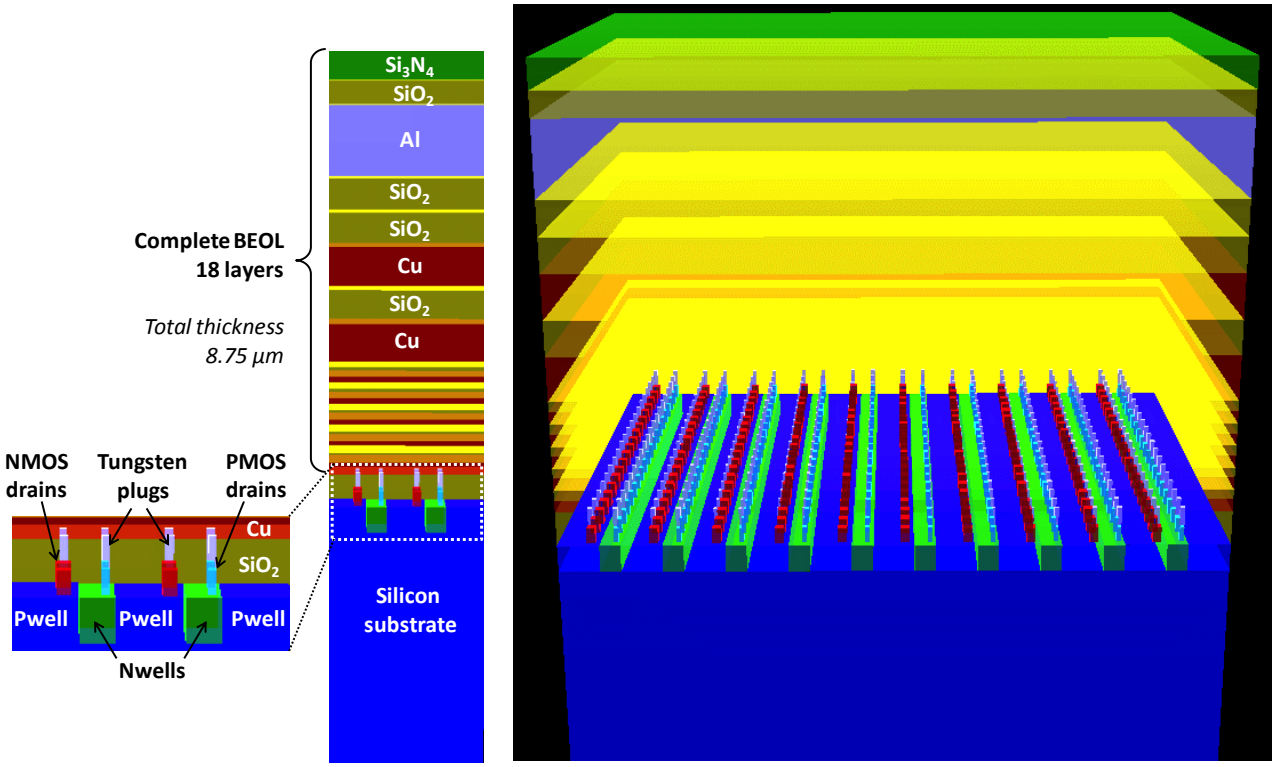

Figure 2. Left and Center: Root screenshots illustrating the geometry of the complete 65 nm SRAM architecture considered in TIARA-G4 simulation. Sensitive PMOS and NMOS drains regions are connected to the first metal layer (Cu) of the BEOL stack with tungsten plugs. The BEOL structure is composed of 18 uniform stacked layers with exact compositions and thicknesses. Right: 3D perspective view of a 10×20 SRAM cell array covered with the BEOL (for better visibility, BEOL layers have been rendered semi-transparent). This 20×10 SRAM cell array is composed of a total of 840 Geant4 objects.

B. Muon physics in Geant4

The physical list used in TIARA-G4 also invokes the following classes and models for the computation of muon interactions and transport. First, the G4MuIonization class provides the continuous energy loss due to muon ionization and simulates the discrete component of the ionization, that is, delta rays (δ–electrons) produced by muons. Inside this class the following models are used:

- The G4BraggIonModel for E < 0.2 MeV. Muon energy losses are derived from the tabulated proton energy loss using scaling relation for the stopping power of heavy particles [25], which is a function only of the particle velocity;
- The G4BetheBlochModel for 0.2 MeV < E < 1 GeV. The Bethe-Bloch formula with shell and density corrections is applied [25].

To handle the muon decay and nuclear muon capture, we respectively invoke the G4MuonDecayChannel and G4MuonMinusCaptureAtRest processes included in any physics lists of Geant4 like QGSP_BIC. In the algorithm of the G4MuonMinusCaptureAtRest process, $\mu^- + p \rightarrow n + \nu_\mu$ reaction is used with the energy conservation. More precisely, the muon is captured by a bound proton with a Fermi momentum of ≈250 MeV/c. The off-shell mass of such a proton is about 45 MeV less than a free proton mass. The muon mass is added to the off-shell mass of the proton and the resulting compound system becomes only about 60 MeV heavier than a free neutron. This compound system decays into a free neutron and a neutrino. The neutrino takes the majority of the energy (about 55 MeV) and the rest of the muon mass (about 50 MeV) is transferred to the nucleus. Nuclear de-excitation is made by the Geant4 Pre-compound model.

C. SRAM construction and simulation in TIARA-G4

We illustrate in this paragraph the construction of the SRAM circuit considered in the present study; we also briefly indicate the electrical criteria used to determine if a memory cell is upset or not by the passage of an ionizing particle. Figure 2 (left) illustrates the geometry of a complete 65 nm SRAM architecture considered in TIARA-G4 simulation. Sensitive Pmos and Nmos drains regions are connected to the first metal layer (Cu) of the BEOL stack with tungsten plugs. The BEOL structure is composed of 18 uniform stacked layers with exact compositions and thicknesses. The 3D perspective view of a 10×20 SRAM cell array covered with the BEOL is shown in Figure 2 (right). For better visibility, BEOL layers have been rendered semi-transparent in this illustration.

Concerning the criteria used to determine the occurrence of cell upset in the memory array, the methodology implemented in TIARA-G4 is based on two distinct electrical criteria:

1) If a single or several charged particles directly pass through a sensitive drain volume, TIARA-G4 directly evaluates from Geant4 data the total energy deposited by these particles in the drain, converts this value into a number of generated electron-hole pairs (Q_{dep}) and finally compares this value with the critical charge values ($Q_{crit,P}$ for Pmos, $Q_{crit,N}$ for Nmos transistors) of the simulated technology. If $Q_{dep} > Q_{crit}$, the memory cell is considered to be upset, in the contrary case, the electrical state of the cell is not changed.

2) If a single or several charged particles impact one or several Nwell, Pwell and/or the silicon substrate, in this case, TIARA-G4 evaluates for each sensitive drain located in the impacted Nwell(s) (for Pmos) or Pwell(s) and substrate (for Nmos) the transient current I(t) resulting from the diffusion of carriers in excess in these regions and the collection of the charge by the sensitive nodes. Such calculations are performed using the "diffusion-collection model" detailed in [22]. Until the I(t) characteristic is computed for all the considered sensitive drains, TIARA-G4 applies the "I_{max}-t_{max}" criterion, also described in [22], to determine if the corresponding memory cell is upset or not.

IV. Simulation results and discussion

For this study, we considered low energy (< 1 MeV) negative and positive muons susceptible to directly deposit charge by ionization or to be captured (negative muons) after they stop in silicon. The Geant4 general particle source was then used to generate mono-energetic muons incident on the 65 nm SRAM architecture (with complete BEOL) previously defined in Section III.C and in Figure 2.

Figure 3 illustrates different possible scenarios of negative and positive muon interactions with the structure. Figure 3(a) shows a negative muon decay in the top layers of the BEOL structure; this cannot lead to an upset since the muon disintegrates in light particles not able to deposit any significant charge in silicon. Figure 3(b) shows a similar event but occurring in the silicon substrate. In this case, the incoming positive muon traverses the complete BEOL structure and, statistically, can cross a sensitive drain. If the charge deposited in the impacted drain is higher than the critical charge for this transistor type and for this technology, the corresponding memory cell is upset. Figures 3 (c) and (d) show two negative muon capture events occurring in the BEOL and in silicon, respectively. These events produce large secondary particle showers, containing one or more charged particles susceptible to reach the active silicon region and to induce an upset or even a multiple cell upset. Of course, the probability to induce an upset is maximum when the muon capture-induce shower is produced in the immediate vicinity of the sensitive drain layer, as illustrated in Figure 3(d). This case corresponds to a reduced energy interval for the incoming muons in so far as the penetration depth of the muons in the structure and then the capture location primarily depends on the muon kinetic energy.

In order to illustrate this effect, we plotted in Figure 4 the distribution inside the SRAM structure of the vertex positions related to the negative muon capture reactions for three different values of the incident muon kinetic energy: 0.1, 0.3 MeV and 0.5 MeV. We clearly evidence in this figure such a dependency of the capture position (depth) with the muon kinetic energy. As a result, the soft error occurrence, and consequently the soft-error rate induced by negative muon irradiation presents a maximum when precisely muon captures occur at the depth of the layer containing sensitive drains (i.e. the active silicon region).

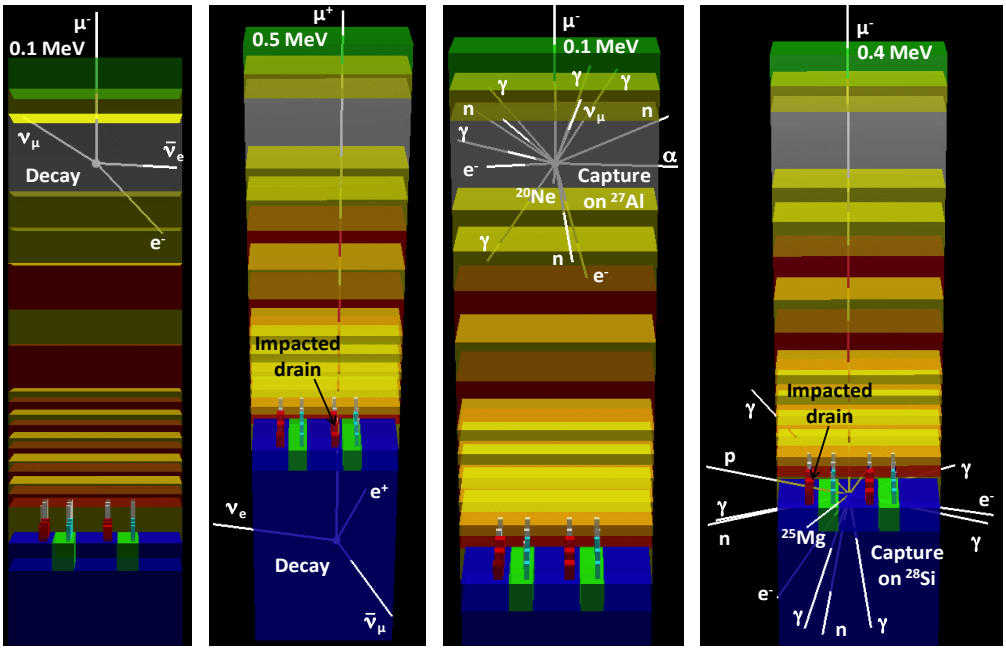

Figure 3. Visualization (Root screenshots) of four events illustrating the interactions of low energy negative and positive muons with the complete SRAM structure. From left to right: μ- decay in the BEOL (Al layer), μ+ upsetting a drain by direct charge deposition though the structure followed by the muon decay in the substrate, μ- capture on an aluminum atom in the BEOL, μ- capture on a silicon atom in the active circuit region (Pwell) leading to a drain upset via a direct impact by a secondary particle (proton in this case).

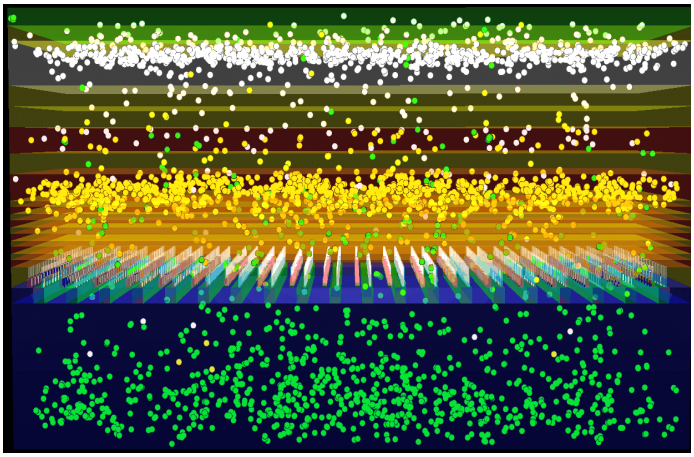

Figure 4. 3D distribution inside the SRAM circuit of the vertex positions related to the negative muon capture reactions for three different values of the incident muon kinetic energy: 0.1 MeV (white dots), 0.3 MeV (yellow dots) and 0.5 MeV (green dots).

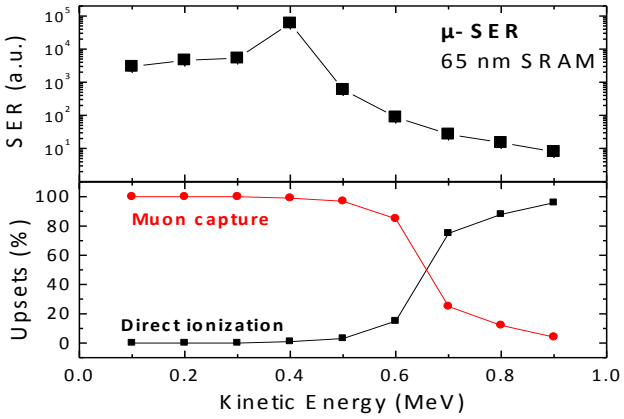

Figure 5. Estimated mono-energetic negative muon-induced soft error rate versus muon kinetic energy for the 65 nm SRAM. The percentage of cell upsets induced by the secondary particles produced by muon capture reactions or directly by muon impacts on sensitive drain (i.e. direct charge deposition in drain volumes) are also plotted.

This behavior is illustrated in Figure 5 which also plots the percentage of cell upsets induced by muon capture reactions or directly by muon impacts on sensitive drain (i.e. direct charge deposition in drain volumes). When increasing the kinetic energy of primary particles, the fraction of upsets induced by muon capture rapidly decreases as soon captures occur deeper in silicon, below the active layer. In this case, upsets become mainly induced by direct charge deposition from incident muons.

The comparison of this simulation result with experimental data previously obtained by Sierawski et al. in [6] is very interesting since it shows similarities in the dependence of the soft-error occurrence with the muon incident kinetic energy.

Figure 1 (top) of Ref. [6] has been obtained for low energy (<3 MeV) positive muons and shows a maximum occurrence of upsets for the tested 65 nm SRAM near 700 keV. At this incident energy, the range of the positive muon beam through the SRAM BEOL is such that a large portion of the muons traversing the active silicon region verify the Bragg peak condition [6]: the deposited charge is then maximum and sufficient to exceed the critical charge of the SRAM under test, leading to a maximum upset rate at this energy. Our simulation result (obtained for a similar but different 65 nm SRAM circuit) shown in Figure 5 is in good agreement with these experimental data, the percentage of upsets induced by negative muons with energies above ~0.7 MeV being

dominated by direct charge deposition. Below this energy, our result evidences an additional mechanism of charge deposition for negative muons resulting from the capture of the incident muons that can be stopped in silicon in the active silicon region. Such an additional channel for muon-induced charge deposition is found to be maximal at 0.4 MeV for the SRAM architecture considered here.

V. Conclusion

This work investigated by numerical simulation using a dedicated code (TIARA-G4) the mechanism of negative muon capture and its effects on the occurrence of SEU in a 65nm SRAM circuit. Our simulation results show that negative muons with energies around 0.4 MeV can be stopped and captured in the vicinity of the sensitive drain region, then inducing upsets via nucleus evaporation which emits charged fragments (mainly Al, Mg, Na ions, protons and alpha particles). Our results complement the recent experimental investigations and simulation results obtained by Sierawski et al. [5-6] concerning the SEU mechanisms induced by positive muons. Future work will try to estimate the exact proportion of positive and negative atmospheric muons that can significantly deposit charge in silicon with respect to not only the circuit architecture but also to the local environment (shielding) of the circuit, susceptible to profoundly impact the distribution of such low energy atmospheric muons below ~1 MeV. The current lack of both experimental and theoretical knowledge related to atmospheric muon distributions below 1 MeV should therefore represent a limitation to accurately estimate the impact of muons on electronics at ground level.

VI. References

[1] J. F. Ziegler and W. A. Lanford, “Effect of cosmic rays on computer memories”. Science, Vol. 206, November 1979.

[2] J. F. Dicello, C. W. McCabe, J. D. Doss, and M. Paciotti, “The relative efficiency of soft-error induction in 4K static RAMs by muons and pions”, IEEE Transactions on Nuclear Science, vol 30, Issue 6, p. 4613-4616, 1983.

[3] C. J. Gelderloos1i, R. J. Peterson, M. E. Nelson, and J. F. Ziegler, “Pion-Induced Soft Upsets in 16 Mbit DRAM Chips”, IEEE Transactions on Nuclear Science, vol 44, Issue 6, p. 2237-2242, 1997.

[4] S. Duzellier, D. Falguère, M. Tverskoy, E. Ivanov, R. Dufayel, and M.-C. Calvet, “SEU Induced by Pions in Memories From Different Generations”, IEEE Transactions on Nuclear Science, vol 48, Issue 6, p. 1960-1965, 2001.

[5] B. D. Sierawski, M. H. Mendenhall, R. A. Reed, M. A. Clemens, R. A. Weller, R. D. Schrimpf, E. W. Blackmore, M. Trinczek, B. Hitti, J. A. Pellish, R. C. Baumann, S.-J. Wen, R. Wong, and N. Tam, “Muon-Induced Single Event Upsets in Deep-Submicron Technology”, IEEE Transactions on Nuclear Science, Vol. 57, No. 6, 2010.

[6] B. D. Sierawski, R. A. Reed, M. H. Mendenhall, R. A. Weller, R. D. Schrimpf, S.-J. Wen, R. Wong, N. Tam, R. C. Baumann, “Effects of Scaling on Muon-Induced Soft Errors”. Reliability Physics Symposium (IRPS), 10-14 April 2011, 2011 IEEE International.

[7] P. Singer, “Emission of particles following muon capture in intermediate and heavy nuclei”. Nuclear Physics, Springer Tracts in Modern Physics, 1974, Volume 71/1974, 39-87, DOI: 10.1007/BFb0041336.

[8] N. C. Mukhopadhyay, “Nuclear Muon capture”. Physics Reports, Volume 30, Issue 1, March 1977, Pages 1–144.

[9] E. Fermi, E. Teller, “The capture of negative mesotrons in matter”. Physical Review, Vol. 72, No 5, September, 1947.

[10] T. Suzuki, D. F. Measday, J. P. Roalsvig, “Total nuclear capture rates for negative muons”. Physical Review C, Vol. 35 No. 6, June 1987.

[11] J. Tiomno, J. A. Wheeler, “Charge-exchange reaction of the μ-meson with the nucleus”. Reviews of Modern Physics, Vol. 21, No. 1, January, 1949.

[12] R. M. Sundelin and R. M. Edelstein, “Neutron Asymmetries and Energy Spectra from Muon Capture in Si, S, and Ca”. Phys. Rev. C 7, 1037–1060 (1973).

[13] S. E. Sobottka and E. L. Wills, “Energy spectrum of charged particles emitted following muon capture in ^{28}Si”. Physical Review Letters, Vol. 20, No. 12, March 1968.

[14] R. M. Sundelin, R. M. Edelstein, a. Suzuki and K. Takahashi, “Spectrum of neutrons from muon capture in silicon, sulfur, and calcium”. Physical Review Letters, Vol. 20, No. 21, May 1968.

[15] B. Macdonald, J. A. Diaz, S. N. Kaplan and R. V. Pyle, “Neutrons from Negative-Muon Capture”. Phys. Rev. 139, B1253–B1263 (1965).

[16] Y. G. Budyashov, V. G. Zinov, A. D. Konin, A. I. Mukhin, A. M. Chatrchyan, “Charged Particles from the Capture of Negative Muons by the Nuclei 28Si, 32S, 40Ca, and 64Cu”. Soviet Journal of Experimental and Theoretical Physics, Vol. 33, p.11 (1971).

[17] A. Wyttenbach, P. Baertschi, S. Bajo, J. Hadermann, K. Junker, S. Katcoff, E.A. Hermes, H.S. Pruys, “Probabilities of muon induced nuclear reactions involving charged particle emission”, Nuclear Physics A, Vol. 294, Issue 3, p. 278–292 (1978).

[18] D.F. Measday, “The nuclear physics of muon capture”. Physics Reports 354 (2001) 243–409.

[19] S. Uznanski, G. Gasiot, P. Roche, C. Tavernier, J-L. Autran, "Single Event Upset and Multiple Cell Upset Modeling in Commercial Bulk 65 nm CMOS SRAMs and Flip-Flops," IEEE Trans. Nucl. Sci., vol. 57, issue 4, Aug 2010.

[20] S. Uznanski, G. Gasiot, P. Roche, J. L. Autran, "Combining GEANT4 and TIARA for Neutron Soft Error Rate Prediction of 65 nm Flip-Flops," IEEE Trans. Nucl. Sci., vol. 58, issue 6, Dec 2011.

[21] S. Agostinelli et al., "Geant4—a simulation toolkit", Nuclear Instruments and Methods in Physics Research Section A: Accelerators, Spectrometers, Detectors and Associated Equipment, Vol. 506, p.250-303, 2003.Geant4 Physics Reference Manual Version: geant4 9.5.0 (2nd December, 2011).

[22] S. Uznanski, “Monte-Carlo simulation and contribution to understanding of Single Event Upset (SEU) mechanisms in CMOS technologies downto 20nm technological node.”, Ph.D. Thesis, Aix-Marseille University, Sept. 2011.

[23] Geant4 General Particle Source, http://reat.space.qinetiq.com/gps/

[24] Geant4 Physics Reference Manual Version: geant4 9.5.0 (December, 2011).

[25] A. Allisy et al., “Stopping Powers and Ranges for Protons and Alpha Particles”, ICRU Rep. 49, 1993.